

## Quantum behavior of a flux qubit coupled to a resonator

A. N. Omelyanchouk

*B. Verkin Institute of Low Temperature Physics and Engineering, National Academy of Sciences of Ukraine, 47 Lenin Ave., 61103 Kharkov, Ukraine*

S. N. Shevchenko<sup>a)</sup>

*B. Verkin Institute of Low Temperature Physics and Engineering, National Academy of Sciences of Ukraine, 47 Lenin Ave., 61103 Kharkov, Ukraine and Institute of Photonic Technology, P.O. Box 100239, D-07702 Jena, Germany*

Ya. S. Greenberg

*Institute of Photonic Technology, P.O. Box 100239, D-07702 Jena, Germany and Novosibirsk State Technical University, 20 Karl Marx Ave., Novosibirsk, 630092, Russia*

O. Astafiev

*NEC Nano Electronics Research Laboratories, Tsukuba, Ibaraki, 305-8501, Japan*

E. Il'ichev

*Institute of Photonic Technology, P.O. Box 100239, D-07702 Jena, Germany*  
(Submitted March 29, 2010)

Fiz. Nizk. Temp. **36**, 1117–1127 (October–November 2010)

A detailed theory for a system of a superconducting qubit coupled to a transmission line resonator is presented. We describe the system by solving analytically and numerically the master equation for the density matrix, which includes a dissipative Lindblad term. We calculate the transmission coefficient, which provides a way to probe the dressed states of a qubit. The theoretical results are related to experiments with intermediate coupling between a qubit and a resonator when the coupling energy is of the same order as the qubit relaxation rate. © 2010 American Institute of Physics. [doi:10.1063/1.3515520]

### I. INTRODUCTION

Contemporary nanotechnology combines quantum optics and mesoscopic solid state physics. The systems currently under extensive investigation include superconducting circuits based on Josephson junctions (Josephson qubits), which are macroscopic quantum objects whose quantum behavior has been demonstrated in experiments (for review see, e.g., Refs. 1–4). Since superconducting qubits are quantum mesoscopic objects, they offer the possibility of observing several unique quantum phenomena, such as entanglement,<sup>5,6</sup> Rabi oscillations,<sup>7–12</sup> spin echo and Ramsey fringes,<sup>13,14</sup> Landau–Zener–Stückelberg interferometry,<sup>15–19</sup> etc. At present there is great interest in the problem of the behavior of artificial atoms in a quantized electromagnetic field in the framework of so-called circuit quantum electrodynamics (CQED).<sup>20</sup> In CQED a superconducting qubit acting as an artificial atom is electrostatically coupled to a high-quality transmission line resonator. The large effective dipole moment of the qubit and the high-energy density of the resonator allow this system to reach the strong coupling limit of CQED in a solid-state system. This idea was proposed recently and has been studied theoretically<sup>21–25</sup> and experimentally for charge qubits that are coupled capacitively to a resonator.<sup>26–28</sup> Inductive coupling of a flux qubit has been proposed<sup>29</sup> and realized.<sup>30,31</sup>

In this paper we consider the quantum state of a complex system consisting of a superconducting flux qubit coupled to

a transmission line resonator. We first give a detailed theory of the qubit's states, dressed by the interaction with the quantum resonator, and their influence on the observable transmittance. We then describe the intermediate coupling regime, which as recently been studied experimentally by Oelsner *et al.*<sup>31</sup> Thus, the paper is organized as follows: a model of the system is presented in the next section. In sec. III we calculate the energy levels of the system, which which matched to the driver photons creates the spectroscopy of this system. The Hamiltonian of the driven system is rewritten in sec. IV in different representations, in particular, in the rotating-wave approximation (RWA) which is convenient for finding the stationary solutions. Solutions of the master equation are given in sec. V: analytic for weak drivers and numerical for strong drivers. The paper ends with Conclusions and an Appendix with details of the theory of the transmittance through the resonator.

### II. DESCRIPTION OF THE SYSTEM

We consider a flux qubit coupled inductively to a quantum resonator (see Fig. 1). The flux qubit is a superconducting loop with three Josephson junctions.<sup>32</sup> The basic states of the qubit correspond to different directions of the current in the loop. The current state of the qubit influences the quantum state of the resonator. We consider a quantum resonator formed between two gaps in the transmission line. The qubit

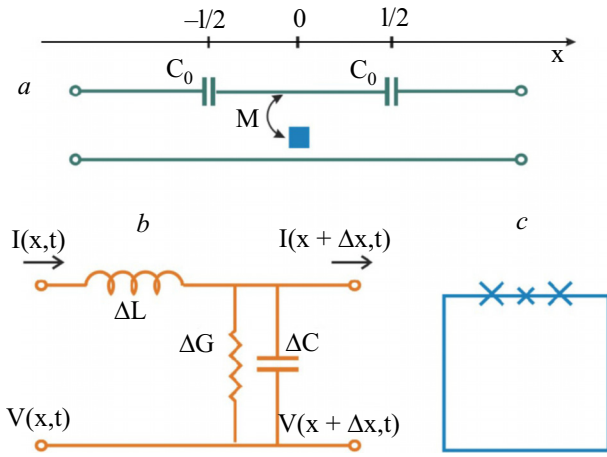


FIG. 1. (Color online) (a) Circuit of a qubit (denoted by the blue box) coupled to a transmission line resonator. (b) Equivalent circuit for an infinitesimal segment of length  $\Delta x$  of the transmission line. (c) A flux qubit with 3 Josephson junctions.

is situated close to the center of the resonator; note that the qubit dimensions are significantly smaller than the resonator wavelength, so we can ignore its size.

The complete Hamiltonian of the driven system, neglecting relaxation processes, is

$$H = H_{\text{qb-r}} + H_{\mu\nu}, \quad (1)$$

where the qubit-resonator Hamiltonian

$$H_{\text{qb-r}} = H_{\text{qb}} + H_r + H_{\text{int}} \quad (2)$$

consists of the bare qubit and resonator terms and the interaction term. The flux qubit Hamiltonian in the flux basis  $\{| \downarrow \rangle, | \uparrow \rangle\}$  is given by<sup>32</sup>

$$H_{\text{qb}} = -\frac{\Delta}{2} \tau_x - \frac{\varepsilon}{2} \tau_z, \quad (3)$$

where  $\Delta$  is the tunnelling amplitude, the energy bias  $\varepsilon = 2I_p(\Phi - \Phi_0/2)$  is defined by the magnetic flux  $\Phi$ ,  $I_p$  is the persistent current,  $\tau_{x,z}$  are Pauli matrices in the flux basis ( $\tau_z | \downarrow \rangle = -| \downarrow \rangle$ ), and the current operator is  $I_{\text{qb}} = -I_p \tau_z$ .

The qubit is assumed to be coupled to the transmission line resonator. The detailed theory is given in the Appendix (see also Refs. 31, 33, and 34). A single-mode resonator is described by the following Hamiltonian:

$$H_r = \hbar \omega_r \left( a^\dagger a + \frac{1}{2} \right), \quad (4)$$

where  $a$  and  $a^\dagger$  are the annihilation and creation operators, which act on the (Fock) number of states in the following way:  $a|n\rangle = \sqrt{n}|n-1\rangle$  and  $a^\dagger|n-1\rangle = \sqrt{n}|n\rangle$ .

The term describing the interaction of the resonator and the flux qubit is

$$H_{\text{int}} = MI(0)I_{\text{qb}} = -\hbar g(a^\dagger + a)\tau_z, \quad (5)$$

where

$$\hbar g = MI_{r0}I_p, \quad (6)$$

$M$  is the mutual inductance, and  $I(0)$  is the transmission line current operator, given by Eq. (74) (see Appendix), at the qubit's position,  $x=0$ .

The transmission line is assumed to be driven by two fields. One is a probing field with amplitude  $V_1^\dagger$  and frequency  $\omega$  close to the resonator characteristic frequency  $\omega_r$ , as described in the Appendix. The amplitude of this field is assumed so small that its effect on the qubit can be neglected. (This is similar to the coupling to a classical resonator considered in Ref. 35, where a low rf current was used to probe a resonator and an ac flux was also applied to drive the qubit.) The other field describes the driving of the qubit with an amplitude  $\xi$  and frequency  $\omega_d$ . The Hamiltonian for this field, described by periodic exchange of photons between the resonator and the driving field, can be written as

$$H_{\mu\nu} = \xi(a^\dagger e^{-i\omega_d t} + a e^{i\omega_d t}). \quad (7)$$

### III. ENERGY LEVELS AND THE SPECTROSCOPY OF DRESSED STATES

We begin by diagonalizing the qubit Hamiltonian, i.e., writing it in the eigenstate representation (see, e.g., Ref. 36). Then the qubit-resonator Hamiltonian can be written (without drive)

$$H'_{\text{qb-r}} = H'_0 + H'_{\text{int}}, \quad (8)$$

$$H'_0 = \frac{\hbar \omega_{\text{qb}}}{2} \sigma_z + \hbar \omega_r \left( a^\dagger a + \frac{1}{2} \right), \quad (9)$$

$$H'_{\text{int}} = -\hbar g(a^\dagger + a) \left( \frac{\varepsilon}{\hbar \omega_{\text{qb}}} \sigma_z - \frac{\Delta}{\hbar \omega_{\text{qb}}} \sigma_x \right), \quad (10)$$

where

$$\hbar \omega_{\text{qb}} = \sqrt{\Delta^2 + \varepsilon^2} \quad (11)$$

is the bare qubit energy difference,  $\sigma_{x,z}$  are Pauli matrices in the energy basis  $\{|g\rangle, |e\rangle\}$  (so that  $\sigma_z |g\rangle = -|g\rangle$ ). The bare system eigenstates are  $|e/g, h\rangle = |e/g\rangle \otimes |n\rangle$  and eigenvalues are

$$E_{e/g,n} = \pm \frac{\hbar \omega_{\text{qb}}}{2} + \hbar \omega_r \left( n + \frac{1}{2} \right). \quad (12)$$

If the frequency  $\omega_r$  is close to the gap frequency of the qubit  $\omega_{\text{qb}}$  (for definitiveness we assume here  $\omega_r > \omega_{\text{qb}}$ ), then for each  $n$  there are pairs of levels  $|e, n\rangle$  and  $|g, n+1\rangle$  which are close in energy. Therefore, in order to find the change in these levels owing to the interaction (10), we include only transitions between these two levels:

$$\langle g, n+1 | H'_{\text{int}} | e, n \rangle = \langle e, n | H'_{\text{int}} | g, n+1 \rangle = \hbar g_\varepsilon \sqrt{n+1}, \quad (13)$$

with

$$g_\varepsilon = g \frac{\Delta}{\hbar \omega_{\text{qb}}}. \quad (14)$$

(Note that away from the degeneracy point ( $\varepsilon=0$ ) the coupling strength is reduced by  $\Delta/\hbar \omega_{\text{qb}}$ .<sup>21</sup>) This leads to new eigenvectors of the Hamiltonian  $H'_{\text{qb-r}}$  which can be written in terms of the eigenvectors of the bare Hamiltonian  $H'_0$  as

$$\begin{pmatrix} |-, n\rangle \\ |+, n\rangle \end{pmatrix} = \begin{pmatrix} \sin \eta & \cos \eta \\ -\cos \eta & \sin \eta \end{pmatrix} \begin{pmatrix} |g, n+1\rangle \\ |e, n\rangle \end{pmatrix}. \quad (15)$$

The solution of the eigenvalue problem is then

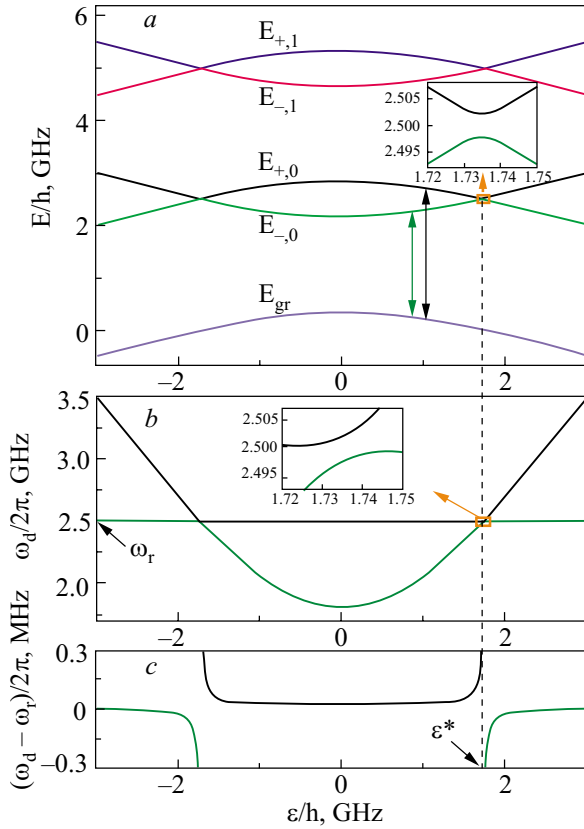


FIG. 2. (Color online) (a) Energy levels as functions of energy bias  $\varepsilon$ . The avoidance of level crossing is illustrated in the magnified inset. The parameters for this and the following figures are:  $\Delta/\hbar=1.8$  GHz,  $g/2\pi=3$  MHz, and  $\omega_r/2\pi=2.5$  GHz. (b) Contours of the energy difference versus bias  $\varepsilon$  and driver frequency  $\omega_d$ . The green (lower) line is for  $\hbar\omega_d=E_{-,0}-E_{gr}$  and the black (upper) line is for  $\hbar\omega_d=E_{+,0}-E_{gr}$ . (c) Same as in (b), but within a very narrow vicinity of the resonator fundamental frequency  $\omega_r$ .

$$\tan 2\eta = \frac{2g_\varepsilon\sqrt{n+1}}{\delta}, \quad (16)$$

$$E_{\pm,n} = \hbar\omega_r(n+1) \pm \frac{\hbar\Omega_n}{2}, \quad (17)$$

$$\Omega_n = \sqrt{4g_\varepsilon^2(n+1) + \delta^2}, \quad (18)$$

$$\delta = \omega_{qb} - \omega_r < 0. \quad (19)$$

The energy of the ground state,  $|g,0\rangle$ , is given by

$$E_{gr} \equiv E_{g,0} = -\frac{\hbar\delta}{2}. \quad (20)$$

Here  $\Omega_n$  determines the difference the energy levels:  $E_{+,n} - E_{-,n} = \hbar\Omega_n$ . In particular, energy anticrossing takes place at  $\delta=0$ , that is at  $\hbar\omega_{qb}(\varepsilon^*) = \hbar\omega_r$ , and it is given by

$$\Omega_n^{\min} = \Omega_n(\varepsilon^*) = 2g_\varepsilon\sqrt{n+1} = 2g\frac{\Delta}{\hbar\omega_r}\sqrt{n+1}. \quad (21)$$

For example, an energy anticrossing for  $n=0$  is shown in the inset of Fig. 2a.

If the cavity is coupled to a weak drive field, one can produce conditions such that only a few lower Fock states of the resonator are relevant (plotted according to Eqs. (17) and (20) in Fig. 2a). This creates the spectroscopy of the

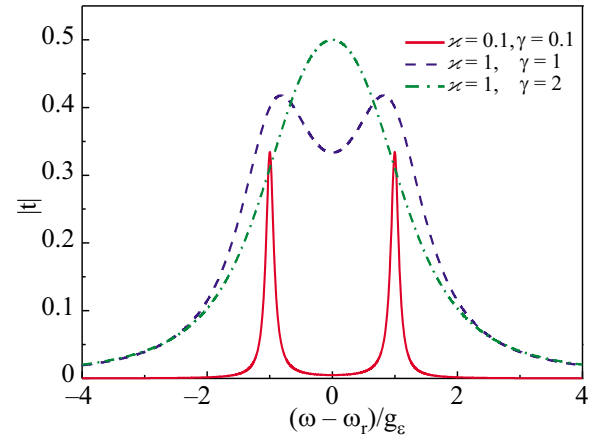


FIG. 3. (Color online) Normalized transmission amplitude  $|t|$  as a function of the driving frequency detuning  $\omega_d - \omega_r$  at  $\varepsilon = \varepsilon^*$  (when  $\omega_{qb}(\varepsilon^*) = \omega_r$ ) for different values of the decay rates  $\varkappa$  and  $\gamma$  (given in the figure in units of  $g_\varepsilon$ ), calculated using Eq. (46).

«dressed» energy levels: the transmission increases resonantly when the drive photon energy  $\hbar\omega_d$  matches the system energy difference from Eqs. (17) and (20); the double arrows in Fig. 2a indicate two possible frequencies. One can then plot the respective energy contours to describe the results of an experiment; see Figs. 2b and 2c, which correspond to the experiment in Figs. 2 and 3 of Ref. 31. If the driver amplitude is increased, one should expect multiphoton transitions involving the upper levels of the qubit, as well (see Refs. 30 and 37).

## IV. SYSTEM HAMILTONIAN

### A. Jaynes–Cummings Hamiltonian

Let us rewrite the interaction Hamiltonian, Eq. (10), by introducing the qubit lowering and raising operators

$$\sigma = \frac{1}{2}(\sigma_x - i\sigma_y) \quad \text{and} \quad \sigma^\dagger = \frac{1}{2}(\sigma_x + i\sigma_y), \quad (22)$$

so that  $\sigma^\dagger|g\rangle = |e\rangle$ ,  $\sigma^\dagger|e\rangle = 0$ , etc.; then we have

$$H'_{\text{int}} = \hbar g_\varepsilon(a^\dagger\sigma + a\sigma^\dagger) + \hbar g_\varepsilon(a\sigma + a^\dagger\sigma^\dagger) - \hbar g\frac{\varepsilon}{\hbar\omega_{qb}}(a^\dagger + a)\sigma_z. \quad (23)$$

The second and the third terms in Eq. (23) can be neglected in the RWA since they do not conserve the number of photons in the system (this will also be justified in the next paragraph). The first term together with  $H'_0$  from Eq. (9) form the Jaynes–Cummings Hamiltonian,

$$H_{JC} = \frac{\hbar\omega_{qb}}{2}\sigma_z + \hbar\omega_r\left(a^\dagger a + \frac{1}{2}\right) + \hbar g_\varepsilon(a^\dagger\sigma + a\sigma^\dagger). \quad (24)$$

### B. Interaction representation

Consider the interaction Hamiltonian  $H'_{\text{int}}$  in the interaction representation. For this we note the following relations (see, e.g.,<sup>38</sup>):

$$e^{ia^\dagger a\omega t} a e^{-ia^\dagger a\omega t} = a e^{-i\omega t}, \quad (25)$$

$$e^{i\omega/2t\sigma_z}\sigma e^{-i\omega/2t\sigma_z} = \sigma e^{-i\omega t}. \quad (26)$$

Then we obtain

$$\begin{aligned} H_{\text{int}}^I &= e^{i\hbar H_0^I t} H_{\text{int}}^I e^{-i\hbar H_0^I t} = \hbar g_\varepsilon (a\sigma^\dagger e^{i(\omega_{\text{qb}} - \omega_r)t} + \text{h.c.}) \\ &+ \hbar g_\varepsilon (a\sigma e^{-i(\omega_{\text{qb}} + \omega_r)t} + \text{h.c.}) - \hbar g \frac{\varepsilon}{\hbar \omega_{\text{qb}}} (a e^{-i\omega t} \\ &+ \text{h.c.}). \end{aligned} \quad (27)$$

In the RWA, when  $\omega_{\text{qb}} - \omega_r \ll \omega_{\text{qb}}$ , the first term is slowly rotating, while the second and third terms are fast rotating ones. This justifies neglecting these terms in the RWA.

### C. Rotating-wave approximation

Consider the Hamiltonian of the driven system in the RWA:

$$H_{\text{RWA}} = U(H_{\text{qb}-r}^I + H_{\mu w})U^\dagger + i\hbar \dot{U}U^\dagger. \quad (28)$$

For this we choose the transformation

$$U = \exp[i\omega_d t (a^\dagger a + \sigma_z/2)] \quad (29)$$

and obtain

$$\begin{aligned} H_{\text{RWA}} &= \hbar \frac{\delta\omega_{\text{qb}}}{2} \sigma_z + \hbar \delta\omega_r a^\dagger a + \hbar g_\varepsilon (a\sigma^\dagger + a^\dagger \sigma) \\ &+ \xi (a^\dagger + a), \end{aligned} \quad (30)$$

$$\delta\omega_{\text{qb}} = \omega_{\text{qb}} - \omega_d,$$

$$\delta\omega_r = \omega_r - \omega_d. \quad (31)$$

### D. With a separate controlling microwave line

For generality, we consider the case in which the qubit is driven by a separate controlling line. Then, instead of Eq. (7), we have

$$H_{\mu w}^{(2)} = -I_p \Phi_{\text{ac}} \cos \omega_d t \cdot \tau_z, \quad (32)$$

where  $\Phi_{\text{ac}}$  is the amplitude of the driver flux. In the qubit eigenstate representation this gives

$$\begin{aligned} H_{\mu w}^{(2)'} &= -I_p \Phi_{\text{ac}} \frac{e^{i\omega_d t} + e^{-i\omega_d t}}{2} \left( \frac{\varepsilon}{\hbar \omega_{\text{qb}}} \sigma_z - \frac{\Delta}{\hbar \omega_{\text{qb}}} \sigma_x \right) \\ &\approx \xi_\varepsilon (e^{i\omega_d t} \sigma + e^{-i\omega_d t} \sigma^\dagger), \end{aligned} \quad (33)$$

$$\xi_\varepsilon = \frac{1}{2} I_p \Phi_{\text{ac}} \frac{\Delta}{\hbar \omega_{\text{qb}}}. \quad (34)$$

Here only slowly rotating terms remain (see the above discussion). Note that the amplitude  $\xi_\varepsilon$  depends on the bias  $\varepsilon$  (see Eq. (11)). Then, after the transformation (29), in the RWA we obtain an expression which differs from Eq. (30) in the replacement of the last term,  $\xi(a^\dagger + a)$ , by  $\xi_\varepsilon(\sigma^\dagger + \sigma)$ .

### E. Dispersive regime

In the dispersive regime (that is, far from resonance, where  $\delta=0$ ) the diagonalization of the Hamiltonian (24) in the second order in  $g/\delta^{38}$  gives

$$H = -\frac{1}{2} \left( \hbar \omega_{\text{qb}} + \frac{\hbar g_\varepsilon^2}{\delta} \right) \sigma_z + \left( \hbar \omega_r + \frac{\hbar g_\varepsilon^2}{\delta} \sigma_z \right) a^\dagger a. \quad (35)$$

This expression shows explicitly how the qubit transition energy is shifted (normalized) by the coupling and, also, how the resonator energy  $\hbar \omega_r$  is shifted in different directions by the qubit, depending on the qubit state.

## V. SOLUTION OF THE MASTER EQUATION FOR THE DENSITY MATRIX OF THE SYSTEM

To describe the dissipative dynamics of the qubit-resonator system, we have to solve the master equation for the density matrix  $\rho$ :

$$\dot{\rho} = -\frac{i}{\hbar} [H, \rho] + \mathcal{L}[\rho]. \quad (36)$$

It includes a dynamic part and a dissipative Lindblad term<sup>39</sup>

$$\mathcal{L}[\rho] = \frac{1}{2} \sum_{k=1}^3 (2C_k \rho C_k^\dagger - C_k^\dagger C_k \rho - \rho C_k^\dagger C_k), \quad (37)$$

where

$$C_1 = \sqrt{\gamma_1} \sigma, \quad \gamma_1 = \frac{1}{T_1},$$

$$C_2 = \sqrt{\frac{\gamma_\phi}{2}} \sigma_z, \quad \gamma_\phi = \frac{1}{T_\phi} = \frac{1}{T_2} - \frac{1}{2T_1},$$

$$C_3 = \sqrt{\varkappa} a. \quad (38)$$

The Lindblad operator  $\mathcal{L}$  describes dissipation (photon decay) in the resonator at a rate  $\varkappa$ , with qubit decoherence having a relaxation rate  $\gamma_1$  and dephasing rate  $\gamma_\phi$ . We consider a nondispersive regime (i.e., near the qubit-resonator resonance). The system Hamiltonian  $H$  in the rotating wave approximation has the form of Eq. (30). The solution of the master equation determines the observable quantities, in particular, the expectation value of the photon field in the resonator

$$\langle a \rangle = \text{Tr}(a\rho). \quad (39)$$

The Hilbert space of the composite system  $H_{QR}$  is the tensor product of the qubit space  $H_Q$  and the photon (resonator) space  $H_R$ , i.e.,  $H_{QR} = H_Q \otimes H_R$  with the basis vectors  $|e/g, n\rangle = |e/g\rangle \otimes |n\rangle$ . The basis vectors  $|g\rangle$  and  $|e\rangle$ , given by

$$|g\rangle = \begin{bmatrix} 1 \\ 0 \end{bmatrix}, \quad |e\rangle = \begin{bmatrix} 0 \\ 1 \end{bmatrix} \quad (40)$$

are the eigenvectors of the operator  $\sigma_z$ . The Fock vectors of the photon field  $|n\rangle$  (the eigenvectors of the photon number operator  $a^\dagger a |n\rangle = n |n\rangle$ ) are vectors in an  $N=\infty$  infinite-dimensional space:

$$|0\rangle = \begin{bmatrix} 1 \\ 0 \\ 0 \\ 0 \\ \vdots \end{bmatrix}, \quad |1\rangle = \begin{bmatrix} 0 \\ 1 \\ 0 \\ 0 \\ \vdots \end{bmatrix}, \quad |2\rangle = \begin{bmatrix} 0 \\ 0 \\ 1 \\ 0 \\ \vdots \end{bmatrix}, \quad \dots \quad |n\rangle = \begin{bmatrix} 0 \\ 0 \\ \vdots \\ 0 \\ \vdots \end{bmatrix}. \quad (41)$$

In terms of the basis  $|e/g, n\rangle$ , the matrix equation (36) is an infinite set of equations for an infinite-dimensional matrix  $\rho_{ij}$ .

In the following we consider the case of  $N=2$ , which allows an analytical solution, and in the case  $N \gg 1$ , we study the problem numerically.

### A. Weak driver limit

To find an analytical solution we restrict the photon space to  $N=2$ , assuming that mean photon number in the resonator (created by a driver field with amplitude  $\xi$ ) is much less than unity. The basis  $|e/g, n\rangle$  in this case consists of 4 basis vectors  $b_i$ :

$$b_1 = |g0\rangle, \quad b_2 = |e0\rangle, \quad b_3 = |g1\rangle, \quad b_4 = |e1\rangle, \quad (42)$$

and the density matrix  $\rho_{ij} = \langle b_i | \rho | b_j \rangle$  takes the form

$$\rho = \begin{pmatrix} \rho_{g0,g0} & \rho_{g0,e0} & \rho_{g0,g1} & \rho_{g0,e1} \\ \rho_{e0,g0} & \rho_{e0,e0} & \rho_{e0,g1} & \rho_{e0,e1} \\ \rho_{g1,g0} & \rho_{g1,g0} & \rho_{g1,g1} & \rho_{g1,e1} \\ \rho_{e1,g0} & \rho_{e1,e0} & \rho_{e1,g1} & \rho_{e1,e1} \end{pmatrix}. \quad (43)$$

In the steady state, Eq. (36) yields 16 linear equations for the matrix elements  $\rho_{ij}$ . In the weak driver limit, on retaining terms up to first order in the amplitude  $\xi$ , we obtain the density matrix  $\rho$ . The nonzero elements of the matrix  $\rho_{ij}$  in the weak driver limit are

$$\begin{aligned} \rho_{g0,g0} &= 1, \\ \rho_{g1,g0} &= \rho_{g0,g1}^* = \frac{\xi(\delta\omega_{qb} - i\gamma)}{g_\varepsilon^2 - (\delta\omega_r - i\kappa/2)(\delta\omega_{qb} - i\gamma)}, \\ \rho_{e0,g0} &= \rho_{g0,e0}^* = \frac{\xi g_\varepsilon}{g_\varepsilon^2 - (\delta\omega_r - i\kappa/2)(\delta\omega_{qb} - i\gamma)}, \end{aligned} \quad (44)$$

where  $\gamma = (\gamma_1/2) + \gamma_\phi$ .

Substituting Eq. (43) in Eq. (39), we obtain the following average value of the photon field in the resonator in the weak driver (WD) limit:

$$\langle a \rangle_{WD} = \frac{\xi(\delta\omega_{qb} - i\gamma)}{g_\varepsilon^2 - (\delta\omega_r - i\kappa/2)(\delta\omega_{qb} - i\gamma)}. \quad (45)$$

The transmitted amplitude of the output driver signal  $|t|$  is determined by the photon field in the resonator and is given by Eq. (100) (see Appendix); in accordance with Eq. (45), we obtain

$$|t|_{WD} = \left| \frac{\kappa}{2} \operatorname{Im} \frac{\delta\omega_{qb} - i\gamma}{g_\varepsilon^2 - (\delta\omega_r - i\kappa/2)(\delta\omega_{qb} - i\gamma)} \right|. \quad (46)$$

We have normalized  $|t|$  to the value when the qubit is decoupled from the resonator,  $g=0$ , with  $\omega_d = \omega_r$ .

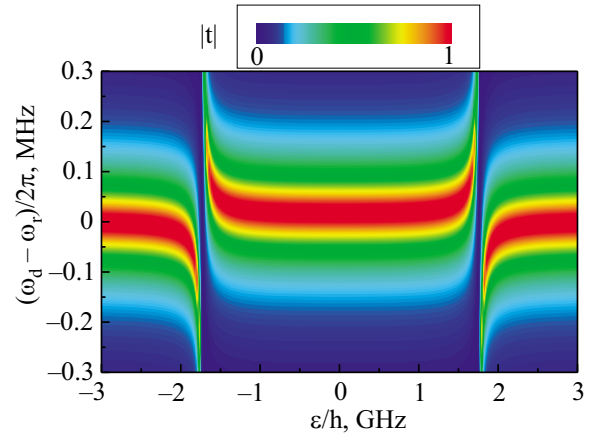


FIG. 4. (Color online) Normalized transmission amplitude  $|t|$  as a function of bias  $\varepsilon$  and driving frequency detuning  $\omega_d - \omega_r$ , calculated using Eq. (46).

The transmission amplitude  $|t|_{WD}$  given by Eq. (46), is plotted in Fig. 3 for  $\omega_{qb} = \omega_r$  and different values of the decay rates  $\kappa$  and  $\gamma$  (given in units of the coupling constant  $g_\varepsilon$ ). For small decay rates  $\kappa$  and  $\gamma$ , the transmission spectrum has Rabi-splitting peaks (solid curve), which spread out with increasing decay.

Figure 4 is a contour plot of the transmission amplitude as a function of the bias  $\varepsilon$  and detuning  $\omega_d - \omega_r$ . The parameters here and in the following have been chosen for comparison with relevant experimental work:<sup>31</sup>  $\Delta/h = 1.8$  GHz,  $g/2\pi = 3$  MHz,  $\omega_r/2\pi = 2.5$  GHz (the same as in Fig. 2), a loss rate in the resonator of  $\kappa/2\pi = 1.25 \cdot 10^{-4}$  GHz, and a loss rate for the qubit of  $\gamma = g$ . Note that we are examining an intermediate coupling regime, where  $g = \gamma \gg \kappa$ . The transmission amplitude increases resonantly along the curves shown in Fig. 2c as expected. The small range of the resonator characteristic frequency,  $\omega_d \in (\omega_r - g, \omega_r + g)$ , makes it possible to avoid a crossing at  $\varepsilon = \varepsilon^*$ , as reported in Ref. 31.

For a more detailed comparison and a determination of the less well known parameters (e.g., the decay rate  $\gamma$ ) it is necessary to compare experimental and theoretical data on the contours of  $|t|$  over  $\varepsilon$  and  $\omega_d$ . This is illustrated in Fig. 5 for  $\omega_d = \omega_r$ .

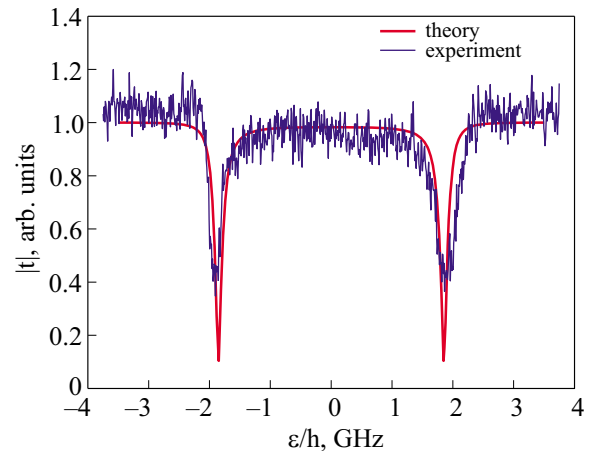


FIG. 5. (Color online) Normalized transmission amplitude  $|t|$  as a function of bias  $\varepsilon$  for  $\omega_d = \omega_r$ , calculated using Eq. (46) and obtained experimentally.

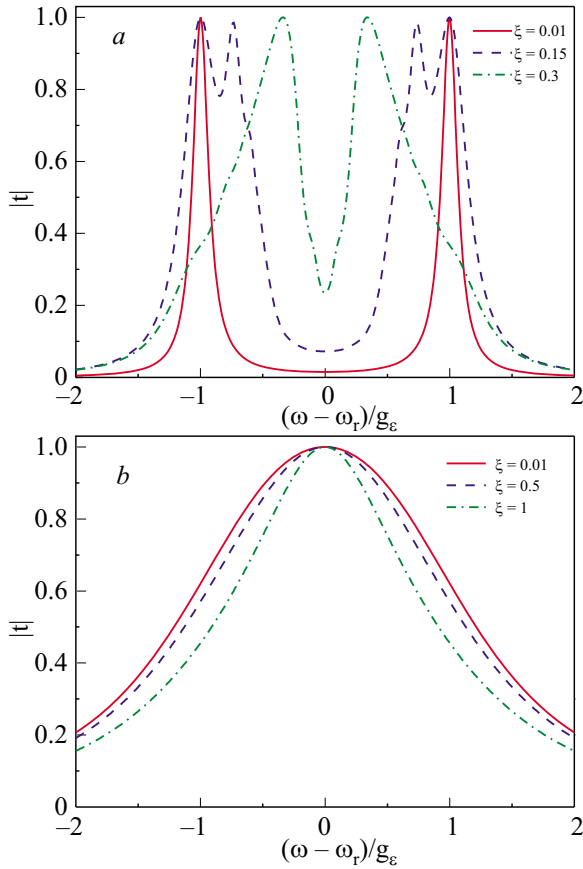


FIG. 6. (Color online) Normalized transmission amplitude  $|t|$  as a function of driving frequency detuning  $\omega_d - \omega_r$  for  $\varepsilon = \varepsilon^*$  (when  $\omega_{qb}(e^*) = \omega_r$ ) for (a)  $\kappa/g_e = 0.1$ ,  $\gamma/g_e = 0.1$  and (b)  $\kappa/g_e = 1$ ,  $\gamma/g_e = 2$ , calculated by numerical solution of the master equation for several values of  $\xi$ , given in units of  $g_e$ .

## VI. NUMERICAL SOLUTION OF THE MASTER EQUATION FOR THE DENSITY MATRIX. BEYOND THE WEAK DRIVER REGIME

In the case of moderate driver amplitudes, i.e., when the mean photon number  $\langle a^\dagger a \rangle \geq 1$ , we have solved the equation for the density matrix  $\rho$  numerically. The results are shown in Fig. 6. The transmission amplitude  $|t|$  in all cases is normalized to the maximum value; as above,  $\omega_{qb} = \omega_r$ . In Fig. 6a the transmission amplitude is shown for the case of small damping:  $\kappa/g_e = 0.1$  and  $\gamma/g_e = 0.1$ . For low driver amplitudes  $\xi$ , the solid curve in Fig. 6a coincides with the dependence  $|t|_{WD}(\omega_d)$  (Fig. 3). With increasing  $\xi$  each split Rabi peak is supersplit (dashed curve) (also, see Ref. 40). With further increases in the amplitude  $\xi$ , this supersplitting is smeared out (dot-dashed curve). Thus, in the nonlinear regime we observe some qualitatively new features compared to the weak driver limit.

When the decay rate is rather high, so that in the weak-driver case Rabi splitting does not occur (dot-dashed curve in Fig. 3), there are no qualitatively new features in the nonlinear response. This is shown in Fig. 6b ( $\kappa/g_e = 1$  and  $\gamma/g_e = 2$ ).

We also calculated the average number of photons in the resonator,  $n = \langle a^\dagger a \rangle$ . For the parameters of Fig. 6 it depends on the frequency; its peak values are  $n_{\max} = 0.005$  for  $\xi/g_e = 0.01$ ,  $n_{\max} = 0.3$  for  $\xi/g_e = 0.15$ , and  $n_{\max} = 1.8$  for  $\xi/g_e = 0.3$ .

## VII. CONCLUSIONS

We given a detailed theory for a system consisting of a flux qubit coupled inductively to a transmission line resonator. The transmission coefficient was calculated using the system's density matrix by solving the master equation in the RWA.

Crossing of the dressed energy levels is avoided in the resonant case, where  $\omega_d \approx \omega_{qb} \approx \omega_r$ . This was demonstrated in the intermediate coupling regime, which corresponds to the experimental results of Oelsner, *et al.*<sup>31</sup> We have shown that dissipation smears out the Rabi splitting. Moreover, we have demonstrated the existence of supersplitting in the strong driver regime.

This work was supported by the State Fund for Fundamental Research, grant F28.2/019, by the EU through the EuroSQIP project, by DFG project IL 150/6-1, and by DAAD scholarship A/10/05536. Ya.S.G. and E.I. acknowledge the financial support of the Federal Agency for Science and Innovation of the Russian Federation under contract No. 02.740.11.5067 and from the Russian Foundation for Basic Research, Grant RFBR-FRSFU No. 09-02-90419. Ya.S.G. and S.N.Sh. thank P. Macha and G. Oelsner for valuable discussions.

## APPENDIX: TRANSMISSION LINE RESONATOR

In this Appendix we consider a resonator formed by a transmission line interrupted by two capacitances  $C_0$ . We assume that a qubit is coupled inductively to the resonator at its center; see Fig. 1a. We begin with the equations for a superconducting transmission line.

### The transmission line

The transmission line can be modelled as an infinite alteration of elementary circuits,<sup>41</sup> as shown in Fig. 1b. Here the elementary inductance, capacitance and conductance are specified per unit length:  $\Delta L = L\Delta x$ ,  $\Delta C = C\Delta x$ ,  $\Delta G = G\Delta x$ .

Looking at the circuit in Fig. 1b, we can write (neglecting Ohmic losses) the circuit equations, by applying the Kirchhoff's laws for the voltage  $V(x, t)$  and the current  $I(x, t)$ ; in the limit  $\Delta x \rightarrow 0$  they take the form

$$\frac{\partial V(x, t)}{\partial x} = -L \frac{\partial I(x, t)}{\partial t}, \quad (47)$$

$$\frac{\partial I(x, t)}{\partial x} = -GV(x, t) - C \frac{\partial V(x, t)}{\partial t}. \quad (48)$$

These equations can be rewritten for either  $I(x, t)$  or  $V(x, t)$  as

$$\frac{\partial^2 A}{\partial x^2} - \frac{1}{v^2} \frac{\partial^2 A}{\partial t^2} = \frac{\kappa}{v^2} \frac{\partial A}{\partial t}, \quad A = \{I, V\}, \quad (49)$$

with

$$v = 1/\sqrt{LC}, \quad (50)$$

$$\kappa = G/C. \quad (51)$$

Here  $v$  has the significance of a phase velocity and  $\kappa$  defines the loss in the transmission line.

Assuming that  $I(x, t) = I(x)e^{i\omega t}$  and  $V(x, t) = V(x)e^{i\omega t}$ , we obtain

$$\frac{dV(x)}{dx} = -i\omega LI(x), \tag{52}$$

$$\frac{dI(x)}{dx} = -(G + i\omega C)V(x). \tag{53}$$

Then the equation for  $A(x) = \{I(x), V(x)\}$  can be written as

$$\frac{d^2 A(x)}{dx^2} - \gamma^2 A(x) = 0, \tag{54}$$

with

$$\gamma = \sqrt{i\omega L(G + i\omega C)} \equiv \alpha + ik. \tag{55}$$

Solving the equation for  $V(x)$  and making use of Eq. (52), we obtain

$$V(x) = V_0^+ e^{-\gamma x} + V_0^- e^{\gamma x}, \tag{56}$$

$$I(x) = \frac{V_0^+}{Z_0} e^{-\gamma x} - \frac{V_0^-}{Z_0} e^{\gamma x}, \tag{57}$$

where

$$Z_0 = \frac{i\omega L}{\gamma} \equiv Z_1 + iZ_2. \tag{58}$$

$$Z_1 = \frac{\omega Lk}{\alpha^2 + k^2}, \quad Z_2 = \frac{\omega L\alpha}{\alpha^2 + k^2}. \tag{59}$$

When the losses in the line are small ( $G \ll \omega C$ ), we have

$$k \approx \omega\sqrt{LC} = \frac{\omega}{v}, \quad \alpha \approx \frac{G}{2} \sqrt{\frac{L}{C}} = \frac{\kappa}{2v}, \tag{60}$$

$$Z_1 = \sqrt{\frac{L}{C}}, \quad Z_2 = \frac{\omega L\alpha}{k^2}. \tag{61}$$

Here the constants  $V_{0+}$  and  $V_{0-}$  stand for the amplitudes of the right- and left-moving waves and  $Z_0$  is the transmission line characteristic (wave) impedance.

### Open transmission-line resonator

Consider an open transmission line of length  $l$ . The quality factor of the resonator can be written as<sup>41</sup>

$$Q = \frac{k}{2\alpha} = \frac{\omega_r C}{G} = \frac{\omega_r}{\kappa}. \tag{62}$$

This equation can be seen as another definition of  $\kappa$ .  $\kappa = \omega_r / Q$ . Let us now determine the normal modes of the resonator without dissipation ( $\kappa = 0$ ). Then, assuming zero current through the boundaries at  $x = \pm l/2$ , we obtain

$$I_j(x) = \frac{V_0^+}{Z_0} (e^{-ik_j x} - (-1)^j e^{ik_j x}), \tag{63}$$

$$V_j(x) = V_0^+ (e^{-ik_j x} + (-1)^j e^{ik_j x}), \tag{64}$$

where  $k_j l = j\pi$ ,  $j = 1, 2, 3, \dots$ . In particular, for the fundamental mode  $j = 1$  of the resonator we obtain

$$I_1(x) = \frac{2V_0^+}{Z_0} \cos k_1 x, \tag{65}$$

$$V_1(x) = -2iV_0^+ \sin k_1 x. \tag{66}$$

For the fundamental mode  $j = 1$  of a  $\lambda/2$  resonator ( $l = \lambda/2$ ), we have  $k_r \equiv k_1 = \pi/l$ ,  $\omega_r \equiv \omega_1 = k_1 v = 2\pi/(2\sqrt{L_r C_r})$ , where  $L_r = Ll$  and  $C_r = Cl$  are the total inductance and capacitance of the resonator.

Let us expand the current in the resonator in terms of the normal modes. We choose the factor in the expansion by analogy with harmonic oscillators (see below):

$$I(x, t) = \sum \sqrt{\frac{2m_j}{L_r}} \omega_j q_j(t) \cos k_j x. \tag{67}$$

For the voltage this gives

$$V(x, t) = -L \int_0^x dx' \frac{\partial I(x', t)}{\partial t} = -\sum \sqrt{\frac{2m_j}{C_r}} \dot{q}_j(t) \sin k_j x. \tag{68}$$

Next, the Hamiltonian is introduced as the total energy of the resonator:

$$H_r = \int_{-l/2}^{l/2} dx \left( \frac{CV^2}{2} + \frac{LI^2}{2} \right) = \frac{1}{2} \sum (m_j \dot{q}_j^2 + m_j \omega_j^2 q_j^2), \tag{69}$$

which coincides formally with the Hamiltonian for a system of harmonic oscillators. This makes it possible to quantize the system with the generalized coordinates  $q_j$  and conjugate momenta  $p_j = m_j \dot{q}_j$ . It is also convenient to introduce the annihilation/creation operators

$$a_j(t) = \frac{m_j \omega_j q_j + ip_j}{\sqrt{2m_j \hbar \omega_j}}, \quad a_j^\dagger(t) = \frac{m_j \omega_j q_j - ip_j}{\sqrt{2m_j \hbar \omega_j}}. \tag{70}$$

In this notation, the current and voltage operators and the Hamiltonian become

$$\hat{I} = \sum \sqrt{\frac{\hbar \omega_j}{L_r}} (a_j + a_j^\dagger) \cos k_j x, \tag{71}$$

$$\hat{V} = i \sum \sqrt{\frac{\hbar \omega_j}{C_r}} (a_j - a_j^\dagger) \sin k_j x, \tag{72}$$

$$\hat{H}_r = \sum \hbar \omega_j \left( a_j^\dagger a_j + \frac{1}{2} \right). \tag{73}$$

In the following we consider a frequency close to the fundamental mode frequency  $\omega_r$ , neglecting the other modes. For the fundamental mode, with  $k_1 = \pi/l$  and omitting the subscript  $j = 1$ , we obtain

$$\hat{I} = I_{r0} (a + a^\dagger) \cos \frac{\pi x}{l}, \quad I_{r0} = \sqrt{\frac{\hbar \omega_r}{L_r}}, \tag{74}$$

$$\hat{V} = iV_{r0} (a - a^\dagger) \sin \frac{\pi x}{l}, \quad V_{r0} = \sqrt{\frac{\hbar \omega_r}{C_r}}, \tag{75}$$

where  $I_{r0}$  and  $V_{r0}$  stand for the zero-point root mean square (rms) current and voltage, and the Hamiltonian is given by Eq. (4). In particular, it follows that at the boundaries  $x$

$= \pm l/2$ , there is no current and the voltage is equal to  $\pm W$ , where

$$W = iV_{r0}\langle a - a^\dagger \rangle = -2V_{r0} \operatorname{Im}\langle a \rangle. \quad (76)$$

### Transmittance of the resonator

Consider now the situation where an input signal is injected into the transmission-line resonator at  $x = -l/2$  through a capacitance  $C_0$  and the output signal is detected after another capacitance  $C_0$  at  $x = l/2$ . We shall obtain a system of equations for  $V_i^+$  and  $V_i^-$ , which determine the classical current and voltage in  $i$ -th region,  $i = 1, 2, 3$ , respectively, for  $x < -l/2$ ,  $x \in (-l/2, l/2)$ , and  $x > l/2$ :

$$V_i(x) = V_i^+ e^{-\gamma x} + V_i^- e^{\gamma x}, \quad (77)$$

$$I_i(x) = \frac{V_i^+}{Z_0} e^{-\gamma x} - \frac{V_i^-}{Z_0} e^{\gamma x}. \quad (78)$$

We assume a matched termination (with impedance equal to  $Z_0$ ), so there is no leftward-propagating wave in the third region, i.e.,  $V_3^- = 0$ . The boundary conditions for the currents and voltages at the points  $x = \pm l/2$  are the following:

$$I_1(-l/2) = I_2(-l/2) \quad (79)$$

$$I_2(l/2) = I_3(l/2), \quad (80)$$

$$V_2(-l/2) = V_1(-l/2) + I_2(-l/2)/i\omega C_0, \quad (81)$$

$$V_3(l/2) = V_2(l/2) + I_3(l/2)/i\omega C_0. \quad (82)$$

For the output signal we obtain  $V_3^+ = V_1^+ t$ ,  $I_3^+ = V_3^+/Z_0 = V_1^+ t/Z_0$ , and

$$t = \frac{4\theta^2}{4\theta^2 + 4i\theta - 1 + e^{-2\gamma l}}, \quad (83)$$

where  $\theta = \omega C_0 Z_0$ .

The phase shift of the output signal relative to the phase of the input signal is  $\phi - kl$ , where  $\phi$  is the phase of  $t$  (Eq. (83)),

$$\tan \varphi = \frac{\operatorname{Im} t}{\operatorname{Re} t}. \quad (84)$$

The transmittance of the resonator is the ratio of the output power at  $x = +l/2$  to the input power at  $x = -l/2$ :

$$T = \frac{P_{\text{out}}}{P_{\text{in}}} = \frac{V_{\text{out}}(l/2)I_{\text{out}}^*(l/2) + V_{\text{out}}^*(l/2)I_{\text{out}}(l/2)}{V_{\text{in}}(-l/2)I_{\text{in}}^*(-l/2) + V_{\text{in}}^*(-l/2)I_{\text{in}}(-l/2)}, \quad (85)$$

where  $V_{\text{in}}(x) = V_1^+ e^{-\gamma x}$ ,  $I_{\text{in}}(x) = I_1^+ e^{-\gamma x}/Z_0$ ,  $V_{\text{out}}(x) = V_3^+ e^{-\gamma x}$ ,  $I_{\text{out}}(x) = I_3^+ e^{-\gamma x}/Z_0$ .

Hence, for the transmittance we obtain

$$T = |t|^2 e^{-2\alpha l}. \quad (86)$$

It is important to note that the losses show up in  $t$  through  $\theta$ , given by

$$\theta = \frac{C_0}{C}(k + i\alpha).$$

If the losses are small ( $\alpha \ll k_2$ ), we can write the transmittance near the first resonance ( $\omega_r = v\pi/l$ ) in the Lorentzian form

$$T = \frac{16\theta_1^4 \omega_r^2}{(2\pi)^2} \left\{ \frac{\omega_r^2}{(2\pi)^2} (4\theta_1^2 + 2\alpha l)^2 + \left[ \frac{\omega_r}{2\pi} (4\theta_1 + 2\alpha l) - \delta\omega \right]^2 \right\}^{-1}, \quad (87)$$

where  $\theta_1 = \omega_r C_0 Z_1$ ,  $\delta\omega = \omega - \omega_r$ .

From Eq. (87) we can see that the main resonance is shifted due to the losses  $\alpha$  and the capacitance  $C_0$ . The width of the Lorentzian profile (87) is given by

$$\Delta\omega = \frac{\omega_r}{\pi} (4\theta_1^2 + 2\alpha l) \quad (88)$$

with a quality factor of

$$Q = \frac{\omega_r}{\Delta\omega} = \frac{\pi}{4\theta_1^2 + 2\alpha l} \quad (89)$$

and transmittance at resonance of

$$T_r = \frac{1}{(1 + \alpha l/2\theta_1)^2}. \quad (90)$$

The first term in (88) defines the photon decay rate  $\kappa$  owing to leakage through the capacitances  $C_0$ ,

$$\kappa = \frac{4\omega_r \theta_1^2}{\pi} = \frac{4\omega_r^2 C_0^2 Z_1}{Cl}. \quad (91)$$

This rate is consistent with the definition given in Ref. 31.

We now estimate the photon decay rate  $\kappa$  for a coplanar waveguide resonator with the parameters in Ref. 42:  $l = 23$  mm,  $\omega_r/2\pi = 2.5$  GHz,  $C_0 = 1$  fF,  $Z_1 = 50$   $\Omega$ . From values yield  $\theta_1 = 7.8 \cdot 10^{-4}$ . The capacitance per unit length  $C$  is calculated from the expression for  $\theta_1$  at resonance,  $\theta_1 = \pi C_0/lC$ . For  $C$  we thus obtain  $C = 1.74 \cdot 10^{-10}$  F/m. Finally, for the photon decay rate, from Eq. (91) we obtain  $\kappa/2\pi = 1.95$  kHz. This value is about half the corresponding experimental values.<sup>42</sup> We assume that the discrepancy is due to dielectric losses associated with  $G$ . This allows us to estimate  $\alpha$  from  $4\theta_1^2 \approx 2\alpha l$  as  $\alpha \approx 5.3 \cdot 10^{-5}$  m<sup>-1</sup>. Therefore, for  $G$  we have  $G = 2\alpha/Z_1 \approx 2.12$   $\Omega^{-1} \cdot \text{m}^{-1}$ .

### Transmittance in the dispersive regime

In the dispersive regime, coupling to the qubit can be described by an additional inductance  $L_q$  at the position  $x = 0$ . This problem involves adding two additional equations for  $x = 0$  to the system of equations (79)–(82). This follows from Eq. (47) on adding the following term to the r.h.s.:

$$-\delta(x)M \frac{\partial I_q}{\partial t} = -\delta(x)L_q \frac{\partial I(x,t)}{\partial t}, \quad (92)$$

where

$$L_q = M^2 \frac{\partial I_q}{\partial \Phi}. \quad (93)$$

In the ground state we have<sup>43,44</sup>

$$L_q = \frac{4M^2 I_p^2 \Delta^2}{(\Delta^2 + \varepsilon^2)^{3/2}}. \quad (94)$$

The solution of the system of equations for the transmission coefficient can be written as follows:

$$t = \left[ \frac{1}{4\theta^2} (e^{-2\gamma l} - (1 - i2\theta)^2) + i \frac{L_q}{8\theta C_0 Z_0^2} (e^{-\gamma l} - 1 + i2\theta)^2 \right]^{-1}. \quad (95)$$

Here the first term describes the transmission without a qubit, i.e., for  $L_q=0$ ; see Eq. (83). This describes resonant transmission (with  $t=1$ ) for

$$\frac{\omega - \omega_r}{\omega_r} = \frac{2\theta}{\pi}. \quad (96)$$

At this frequency the transmission phase (84) is

$$\tan \varphi = - \frac{1}{2\pi} \left( \frac{C_r}{C_0} \right)^2 \frac{L_q}{L_r}, \quad (97)$$

where we have assumed  $C_r L_q / C_0 L_r \ll 1$ . In the ground state we obtain

$$\tan \varphi = -A [1 + (\varepsilon/\Delta)^2]^{-3/2}, \quad (98)$$

with

$$A = \frac{2}{\pi} \left( \frac{C_r}{C_0} \right)^2 \frac{\hbar g^2}{\omega_r \Delta}. \quad (99)$$

### Transmittance in the resonant regime

The solution of the system of equations (79)–(82) can also be used to write the transmission in terms of the field in the resonator:  $V_3^+ = i2\theta e^{\gamma l} V_2^-$ ; then after the quantization of the field in the resonator (see Eq. (76)) we arrive at an expression for  $t = V_3^+ / V_1^+$ ,

$$t = 2\theta \frac{W}{V_1^+} = -\kappa \frac{\text{Im}\langle a \rangle}{2\xi}, \quad (100)$$

which relates the transmission coefficient  $t$  to the photon field  $\langle a \rangle$ . Here we have used the fact that  $\xi = C_0 V_{r0} V_1^+ / 2$  in Eq. (7).

<sup>a</sup>Email: sshevchenko@ilt.kharkov.ua

<sup>1</sup>E. Il'ichev, A. Yu. Smirnov, M. Grajcar, A. Izmalkov, D. Born, N. Oukhanski, Th. Wagner, W. Krech, H.-G. Meyer, and A. Zagoskin, *Fiz. Nizk. Temp.* **30**, 823 (2004) [*Low Temp. Phys.* **30**, 620 (2004)].  
<sup>2</sup>J. Q. You and F. Nori, *Phys. Today* **58**(11), 42 (2005).  
<sup>3</sup>G. Wendin and V. S. Shumeiko, arXiv:cond-mat/0508729; *Fiz. Nizk. Temp.* **33**, 957 (2007) [*Low Temp. Phys.* **33**, 724 (2007)].  
<sup>4</sup>A. Zagoskin and A. Blais, *Phys. Canada* **63**, 215 (2007).  
<sup>5</sup>Yu. A. Pashkin, T. Yamamoto, O. Astafiev, Y. Nakamura, D. V. Averin, and J. S. Tsai, *Nature* **421**, 823 (2003).  
<sup>6</sup>A. Izmalkov, M. Grajcar, E. Il'ichev, Th. Wagner, H.-G. Meyer, A. Yu. Smirnov, M. H. S. Amin, Alec Maassen van den Brink, and A. M. Zagoskin, *Phys. Rev. Lett.* **93**, 037003 (2004).  
<sup>7</sup>D. Vion, A. Aassime, A. Cottet, P. Joyez, H. Pothier, C. Urbina, D. Esteve, and M. H. Devoret, *Science* **296**, 886 (2002).  
<sup>8</sup>I. Chiorescu, Y. Nakamura, C. J. P. M. Harmans, and J. E. Mooij, *Science* **299**, 1869 (2003).  
<sup>9</sup>I. Chiorescu, P. Bertet, K. Semba, Y. Nakamura, C. J. P. M. Harmans, and

J. E. Mooij, *Nature* **431**, 160 (2004).  
<sup>10</sup>E. Il'ichev, N. Oukhanski, A. Izmalkov, Th. Wagner, M. Grajcar, H.-G. Meyer, A. Yu. Smirnov, Alec Maassen van den Brink, M. H. S. Amin, and A. M. Zagoskin, *Phys. Rev. Lett.* **91**, 097906 (2003).  
<sup>11</sup>J. Johansson, S. Saito, T. Meno, H. Nakano, M. Ueda, K. Semba, and H. Takayanagi, *Phys. Rev. Lett.* **96**, 127006 (2006).  
<sup>12</sup>A. N. Omelyanchouk, S. Savel'ev, A. M. Zagoskin, E. Il'ichev, and F. Nori, *Phys. Rev. B* **80**, 212503 (2009).  
<sup>13</sup>Y. Nakamura, Yu. A. Pashkin, T. Yamamoto, and J. S. Tsai, *Phys. Rev. Lett.* **88**, 047901 (2002).  
<sup>14</sup>D. Vion, A. Aassime, A. Cottet, P. Joyez, H. Pothier, C. Urbina, D. Esteve, and M. H. Devoret, *Fortschr. Phys.* **51**, 462 (2003).  
<sup>15</sup>A. Izmalkov, M. Grajcar, E. Il'ichev, N. Oukhanski, Th. Wagner, H.-G. Meyer, W. Krech, M. H. S. Amin, Alec Maassen van den Brink, and A. M. Zagoskin, *Europhys. Lett.* **65**, 844 (2004).  
<sup>16</sup>W. D. Oliver, Ya. Yu, J. C. Lee, K. K. Berggren, L. S. Levitov, and T. P. Orlando, *Science* **310**, 1653 (2005).  
<sup>17</sup>M. Sillanpää, T. Lehtinen, A. Paila, Yu. Makhlin, and P. Hakonen, *Phys. Rev. Lett.* **96**, 187002 (2006).  
<sup>18</sup>S. N. Shevchenko, S. Ashhab, and F. Nori, *Phys. Rep.* **492**, 1 (2010).  
<sup>19</sup>G. Sun, X. Wen, B. Mao, J. Chen, Y. Yu, P. Wu, and S. Han, *Nat. Commun.* **1**, 51 (2010).  
<sup>20</sup>R. J. Schoelkopf and S. M. Girvin, *Nature* **451**, 664 (2008).  
<sup>21</sup>A. Blais, R.-S. Huang, A. Wallraff, S. M. Girvin, and R. J. Schoelkopf, *Phys. Rev. A* **69**, 062320 (2004).  
<sup>22</sup>Y. X. Liu, C. P. Sun, and F. Nori, *Phys. Rev. A* **74**, 052321 (2006).  
<sup>23</sup>Y.-L. Chen, Y.-F. Xiao, X. Zhou, Xu-Bo Zou, Z.-W. Zhou, and G.-C. Guo, *J. Phys. B* **41**, 175503 (2008).  
<sup>24</sup>J. Bourassa, J. M. Gambetta, A. A. Abdumalikov, Jr., O. Astafiev, Y. Nakamura, and A. Blais, *Phys. Rev. A* **80**, 032109 (2009).  
<sup>25</sup>S. Ashhab and F. Nori, *Phys. Rev. A* **81**, 042311 (2010).  
<sup>26</sup>A. Wallraff, D. I. Schuster, A. Blais, L. Frunzio, R.-S. Huang, J. Majer, S. Kumar, S. M. Girvin, and R. J. Schoelkopf, *Nature* **431**, 162 (2004).  
<sup>27</sup>D. I. Schuster, A. Wallraff, A. Blais, L. Frunzio, R.-S. Huang, J. Majer, S. M. Girvin, and R. J. Schoelkopf, *Phys. Rev. Lett.* **94**, 123602 (2005).  
<sup>28</sup>D. I. Schuster, *Circuit Quantum Electrodynamics*, PhD thesis, Yale University (2007).  
<sup>29</sup>T. Lindström, C. H. Webster, J. E. Healey, M. S. Colclough, C. M. Muirhead, and A. Y. Tzalenchuk, *Supercond. Sci. Technol.* **20**, 814 (2007).  
<sup>30</sup>A. A. Abdumalikov, Jr., O. Astafiev, Y. Nakamura, Yu. A. Pashkin, and J. S. Tsai, *Phys. Rev. B* **78**, 180502(R) (2008).  
<sup>31</sup>G. Oelsner, S. H. W. van der Ploeg, P. Macha, U. Hübner, D. Born, S. Anders, E. Il'ichev, H.-G. Meyer, M. Grajcar, S. Wünsch, M. Siegel, A. N. Omelyanchouk, and O. Astafiev, *Phys. Rev. B* **81**, 172505 (2010).  
<sup>32</sup>T. P. Orlando, J. E. Mooij, L. Tian, C. H. van der Wal, L. S. Levitov, S. Lloyd, and J. J. Mazo, *Phys. Rev. B* **60**, 15399 (1999).  
<sup>33</sup>O. Astafiev, A. M. Zagoskin, A. A. Abdumalikov, Jr., Yu. A. Pashkin, T. Yamamoto, K. Inomata, Y. Nakamura, and J. S. Tsai, *Science* **327**, 840 (2010).  
<sup>34</sup>L. Zhou, Z. R. Gong, Y. X. Liu, C. P. Sun, and F. Nori, *Phys. Rev. Lett.* **101**, 100501 (2008).  
<sup>35</sup>S. N. Shevchenko, S. H. W. van der Ploeg, M. Grajcar, E. Il'ichev, A. N. Omelyanchouk, and H.-G. Meyer, *Phys. Rev. B* **78**, 174527 (2008).  
<sup>36</sup>Ya. S. Greenberg, *Phys. Rev. B* **76**, 104520 (2007).  
<sup>37</sup>J. M. Fink, M. Göppl, M. Baur, R. Bianchetti, P. J. Leek, A. Blais, and A. Wallraff, *Nature* **454**, 315 (2008).  
<sup>38</sup>W. P. Schleich, *Quantum Optics in Phase Space*, Wiley-VCH, Berlin (2001).  
<sup>39</sup>M. O. Scully and M. S. Zubairy, *Quantum Optics*, Cambridge, Cambridge University Press (1997).  
<sup>40</sup>L. S. Bishop, J. M. Chow, J. Koch, A. A. Houck, M. H. Devoret, E. Thuneberg, S. M. Girvin, and R. J. Schoelkopf, *Nat. Phys.* **5**, 105 (2009).  
<sup>41</sup>D. M. Pozar, *Microwave Engineering*, Wiley, New York, 3rd ed. (1990).  
<sup>42</sup>P. Macha, S. H. W. van der Ploeg, G. Oelsner, E. Il'ichev, H.-G. Meyer, S. Wünsch, and M. Siegel, *Appl. Phys. Lett.* **96**, 062503 (2010).  
<sup>43</sup>Ya. S. Greenberg, A. Izmalkov, M. Grajcar, E. Il'ichev, W. Krech, H.-G. Meyer, M. H. S. Amin, and A. Maassen van den Brink, *Phys. Rev. B* **66**, 214525 (2002).  
<sup>44</sup>M. Grajcar, A. Izmalkov, E. Il'ichev, Th. Wagner, N. Oukhanski, U. Hübner, T. May, I. Zhilyaev, H. E. Hoenig, Ya. S. Greenberg, V. I. Shnyrkov, D. Born, W. Krech, H.-G. Meyer, Alec Maassen van den Brink, and M. H. S. Amin, *Phys. Rev. B* **69**, 060501(R) (2004).

This article was published in English in the original Russian journal. Reproduced here with stylistic changes by AIP.